HEELING MOMENT ACTING ON A RIVER CRUISER IN MANOEUVRING MOTION

Tomasz Tabaczek, Ph. D.
Jan Kulczyk, Prof.
Wrocław University of Technology, Poland

ABSTRACT

By using fully theoretical method the heeling moment due to centrifugal forces has been determined for a small river cruiser in turning manoeuvre. The authors applied CFD software for determination of hull hydrodynamic forces, and open water characteristics of ducted propeller for estimation of thrust of rudder-propellers. Numerical integration of equations of 3DOF motion was used for prediction of ship trajectory and time histories of velocities, forces and heeling moment.

INTRODUCTION

Regulations that apply to new ships require that properties referring to stability and manoeuvrability must be proved prior to ship construction. In the case of conventional ships standard calculations of stability are carried out and external loads are estimated by using the appropriate formulae, usually given in rules of ship classification. In the cases of non-conventional ships or non-conventional ship equipment more sophisticated methods are required to evaluate loads for stability calculations.
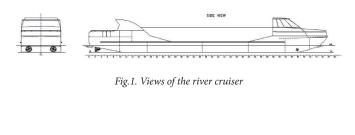
The Directive of the European Parliament on technical requirements for inland waterway vessels [1], in the article on stability says that for passenger vessels driven by rudder-propellers the heeling moment due to centrifugal force (M_{dr}), caused by the turning of the vessel „shall be derived from full-scale or model tests or else from corresponding calculations".

In the case of inland waterway vessels the model tests are usually not commissioned due to the relatively high cost. Full scale trials are possible only when the ship is launched and equipped. Thanks to development of theoretical methods and computational technology the „corresponding calculations" became an actual alternative.

The present authors used the equations of ship planar motion to simulate the turning manoeuvre and to determine the heeling moment acting on a small river cruiser. Data of the considered vessel were provided by Navishipproject , the ship design company of Wrocław. Ship is propelled and controlled by two rudder-propellers and a transverse bow thruster. In order to determine the heeling moment due to centrifugal force the turning manoeuvres have been simulated in deep water, at approach speed of 11 knots (5.66 m/s; Fn = 0.295), after sudden turning of both propulsors 35, 60 and 90 deg

to starboard. In the extreme case of 90 deg even the action of the bow thruster was considered.

RIVER CRUISER

General view and body plan of the considered vessel are shown in Fig. 1 and 2. Its main dimensions are given in Tab. 1. For enhanced manoeuvrability the ship was equipped with two rudder-propellers in nozzles and a tunnel bow thruster.
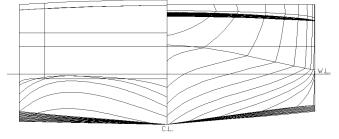

Fig.1. Views of the river cruiser

Fig.2. Body plan of the river cruiser

Tab. 1: Main dimensions of the cruiser

Length overall, L_{OA} [m]	39.00
Length between perpendiculars, L_{PP} [m]	37.63
Breadth, B [m]	6.48
Draught, d [m]	1.10
Rudder-propellers	
No. of blades, z	4
Diameter, D [m]	0.85
Pitch- to- diameter ratio, P/D	0.98
Expanded area ratio, A_E/A_0	0.70

EQUATIONS OF MANOEUVRING MOTION

Ship trajectory and heading were described in the Earth-fixed coordinate system O_{x0y0}. Equations of motion were written in the coordinate system Gxy fixed to moving ship, with its origin at longitudinal position of ship's centre of gravity G (Fig.3). The assumptions were made that heel angle during manoeuvres is small, dynamic trim and sinkage in deep water can be neglected, and, consequently, only 3 degrees of freedom corresponding to surge, sway and yaw motions were considered.

The assumption of negligible small heel angle (i.e. such small that it does not affect the manoeuvring motion) was made because basic data for solving the equation of roll motion, i.e. the moment of inertia of ship around the longitudinal axis was not available (the seakeeping analysis is usually not performed for inland waterway vessels). The assumption was justified by the relatively big value of metacentric height of 2.7 m for the considered river cruiser. The validity of the assumption was proved by calculations of static and dynamic stability after the simulations are completed and heeling moments are known. Predicted values of heel angle during the turning circle manoeuvre are presented in the section 'Results of simulations'.
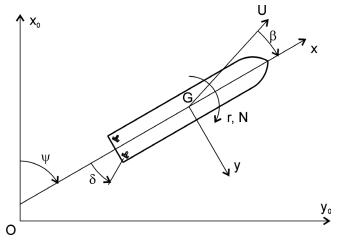

Fig.3. Coordinate systems used in mathematical description of ship motion

$$m (du/dt - vr) = X$$
$$m (dv/dt + ur) = Y \quad \textbf{(1)}$$
$$I_{zz} dr/dt = N$$

where u and v denote the longitudinal and transverse components of the ship velocity U,

r -yaw rate,
X, Y -components of external force,
N -external moment,
m -ship's mass,
I_{zz} -ship's moment of inertia.

The MMG modular model [2] was adapted for external forces and moment:

$$X = -m_x du/dt + m_y vr + X_H + X_P + X_{BT}$$
$$Y = -m_y dv/dt - m_x ur + Y_H + Y_P + Y_{BT} \quad \textbf{(2)}$$
$$N = -J_{zz} dr/dt + N_H + N_P + N_{BT}$$

Subscripts „H", „P" and „BT" refer to hull, propeller and bow thruster, respectively. Inertia forces due to added mass, although of hydrodynamic nature, are written as separate terms. After substitution and rearrangement the equations of motion take the following form, ready for integration:

$$(m + m_x)du/dt - (m + m_y)vr = X_H + X_P + X_{BT}$$
$$(m + m_y)dv/dt + (m + m_x)ur = Y_H + Y_P + Y_{BT} \quad \textbf{(3)}$$
$$(I_{zz} + J_{zz})dr/dt = N_H + N_P + N_{BT}$$

HULL FORCES X_H, Y_H AND MOMENT N_H

The hull forces X_H, Y_H and moment N_H are approximated with the following mathematical models with hydrodynamic coefficients given in Tab. 2:

$$X_H = 0.5\rho LdU^2 X'_H = 0.5\rho LdU^2 (X'_0 + X'_\beta\beta + X'_r r' + X'_{\beta\beta}\beta^2 + X'_{\beta r}\beta r' + X'_{rr}r'^2)$$

$$Y_H = 0.5\rho LdU^2 Y'_H = 0.5\rho LdU^2 (Y'_\beta\beta + Y'_r r' + Y'_{\beta\beta}\beta^2 + Y'_{\beta r}\beta r' + Y'_{rr}r'^2 + Y'_{\beta\beta\beta}\beta^3 + Y'_{\beta\beta r}\beta^2 r' + Y'_{\beta rr}\beta r'^2 + Y'_{rrr}r'^3) \quad \textbf{(4)}$$

$$N_H = 0.5\rho L^2 dU^2 N'_H = 0.5\rho L^2 dU^2 (N'_\beta\beta + N'_r r' + N'_{\beta\beta}\beta^2 + N'_{\beta r}\beta r' + N'_{rr}r'^2 + N'_{\beta\beta\beta}\beta^3 + N'_{\beta\beta r}\beta^2 r' + N'_{\beta rr}\beta r'^2 + N'_{rrr}r'^3)$$

where r' denotes the non-dimensional yaw rate: r' = rL/U.

Tab. 2.: Hydrodynamic coefficients for mathematical model of hull forces and moment

X'_0	-0.02575				
X'_β	-0.02012	Y'_β	0.23166	N'_β	0.02182
X'_r	-0.01389	Y'_r	0.06128	N'_r	-0.02233
$X'_{\beta\beta}$	-0.00364	$Y'_{\beta\beta}$	0.42991	$N'_{\beta\beta}$	0.05866
$X'_{\beta r}$	0.01889	$Y'_{\beta r}$	0.16341	$N'_{\beta r}$	-0.06085
X'_{rr}	0.00128	Y'_{rr}	0.00655	N'_{rr}	-0.02639
		$Y'_{\beta\beta\beta}$	-0.17774	$N'_{\beta\beta\beta}$	-0.04237
		$Y'_{\beta\beta r}$	-0.18127	$N'_{\beta\beta r}$	-0.04646
		$Y'_{\beta rr}$	0.11507	$N'_{\beta rr}$	0.01736
		Y'_{rrr}	0.00209	N'_{rrr}	0.00087

In order to determine the hydrodynamic coefficients a series of computations was carried out by using RANSE-CFD software. Ship flow in steady motion was computed in full scale of vessel, including yaw with drift combinations.

Only positive value of drift angle and yaw rate were considered because negative values were not expected during the starboard turning manoeuvre.

It was expected that the greatest heeling moment appears when the rudder-propellers are set to δ = 90 deg, the ship turns and moves almost sideway. Then the model of hydrodynamic forces should be extended to high drift angles (ß ≤ 90 deg). However, during preliminary simulations of ship motion in turning manoeuvre it was revealed that yaw rate grows quickly (see Fig.6). Problems were encountered during CFD computations of steady ship flow at yaw rates r' > 1.6 due to the effect of memory (ship encounters her own wake before steady flow is attained). These authors decided to confine the model of hydrodynamic forces to r' ≤ 1.6 and ß ≤ 50 deg (Fig.4). Consequently, the simulations of ship motion were stopped when the non-dimensional yaw rate exceeded the value of r' = 1.6. As seen in Fig.6, the computation of hydrodynamic coefficients at drift angles higher than 50 deg was not necessary.

Mathematical models (4) were adopted for good approximation of forces and moment in possibly widest range of drift angle and yaw rate. Coefficients were determined by fitting the models to computed forces. In the case of Y_H and N_H the fitting is excellent (Fig.4). The fitting of surge force X_H is good, at least for drift angles and yaw rates that occur during simulated manoeuvres, shown in Fig.6.
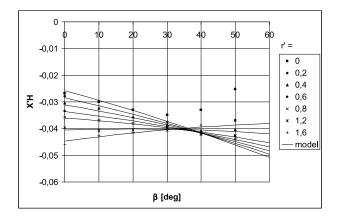
Added masses and added moment of inertia were approximated by using formulae developed by Yasukawa et al. [3] for barge trains of similar proportions of main dimensions (0.012 ≤ d/L ≤ 0.027; 0.048 ≤ B/L ≤ 0.317; 3.89 ≤ B/d ≤ 11.68):

$$m_x = 0.5\rho L^2 d \,(0.151\, B/L - 0.244\, d/L - 0.0012\, B/d + 0.0018)$$
$$m_y = 0.5\rho L^2 d \,(2.93\, d/L + 0.0226)$$
$$J_{zz} = 0.5\rho L^4 d \,(0.0978\, d/L + 0.0025)$$

The values estimated for river uiser (d/L = 0,029, B/L = 0,172, B/d = 5,89) are presented in Tab. 3.

Tab. 3. Added masses and moment of inertia estimated for the river cruiser

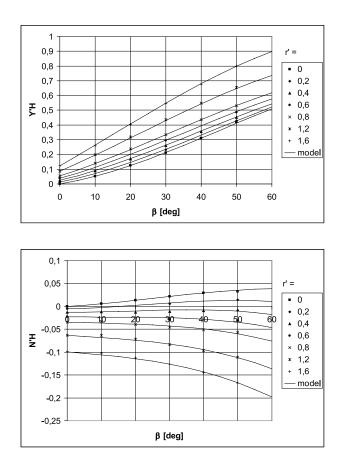| m_x = 10 600 kg	m_x/m = 0,056
m_y = 84 300 kg	m_y/m = 0,45
J_{zz} = 5 910 000 kgm^2	J_{zz}/I_{zz} = 0,30

Fig.4. Fitting of the mathematical model to calculated hull forces and moment

PROPELLER FORCES X_P, Y_P AND MOMENT N_P

Azimuthing thrusters used as rudder-propellers can generate thrust in arbitrary direction determined by steering angle. In contrast to conventional propellers, the terms YP and NP in mathematical model become significant. The authors applied the following formulae for estimation of propeller forces and moment. Inflow to propellers is determined by local drift angle. It was assumed, similar as in the case of conventional rudders [2], that ship's wake affects only the longitudinal inflow to propeller. Flow straightening effect of hull affecting the transverse component of inflow velocity, was neglected.

In the case of twin propeller ship each propeller force in external force model (2) is the sum of forces due to port side and starboard propeller:

$$X_P = X_P^{(p)} + X_P^{(s)}$$
$$Y_P = Y_P^{(p)} + Y_P^{(s)}$$
$$N_P = N_P^{(p)} + N_P^{(s)}$$

(5)

For individual propeller (Fig.5):

$$X_P^{(p,s)} = FP\cos\delta$$
$$Y_P^{(p,s)} = -FP\sin\delta$$
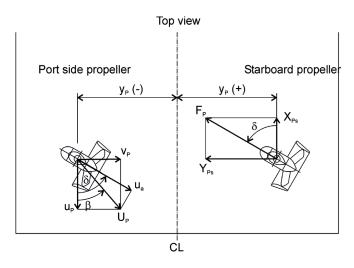$$N_P^{(p,s)} = -XP^{(p,s)}yP^{(p,s)} + YP^{(p,s)}xP^{(p,s)}$$

(6)

Top view

Fig.5. Forces generated by rudder-propellers

where the net force due to propeller action FP is determined separately for each propeller (component perpendicular to propeller axis caused by oblique inflow to propeller was not considered):

$$F_P = (1-t) \, K_T \, \rho n^2 D^4 - \Delta T$$

$$
\begin{aligned}
J &= u_a \, / \, nD \\
u_a &= u_p \cos\delta - v_p \sin\delta \\
u_p &= u(1-w) \\
v_p &= v + x_p r
\end{aligned}
\tag{7}
$$

F_P -net force due to propeller action,
δ –steering angle,
x_P, y_P -horizontal coordinates of steering column,
t -thrust deduction factor,
K_T -thrust coefficient, approximated by using open water propeller characteristics $K_T(J)$,
ρ -water density,
n -propeller revolutions,
D -propeller diameter.
ΔT -loss of thrust due to presence of steering column,
J -propeller advance coefficient,
u_a -axial component of propeller inflow velocity
u_p, v_p -longitudinal and transverse components of propeller inflow velocity,
w -effective wake fraction.

For the purpose of the present simulations the open water characteristics of rudder-propeller was approximated with open water characteristics of corresponding ducted propeller from the Wageningen Ka4-70 screw series in nozzle 19A [4]:

$$K_T(J) = -0.3911 \, J^3 + 0.2727 \, J^2 - 0.5869 \, J + 0.5078 \tag{8}$$

Based on estimated resistance curve the propeller revolutions were adjusted to 11.4 rps to provide the approach speed of 5.66 m/s. Thrust deduction factor of 0.15 and wake fraction of 0.12 were assumed as reasonable values for ship hull with stern tunnels and azimuthing thrusters in deep water.

BOW THRUSTER FORCE Y_{BT} AND MOMENT N_{BT}

Bow thrusters are usually used when ship is manoeuvring at zero- or low speed. However, to be on the safe side, these authors considered a hypothetical case of using bow thruster at cruising speed of 11 kn.

The performance of transverse tunnel thrusters depends both on hull form of ship (on geometry of bow in the case of bow thrusters), as well as on the parameters of motion (speed and drift angle) [5]. The interaction of jet from the thruster with ship flow results in additional hydrodynamic forces acting on the hull. The lateral thruster performance rapidly decreases at non-zero ship speeds. In order to account for the variation of forces and steering moment due to bow thruster in manoeuvring motion the appropriate characteristics of thruster performance are required. Unfortunately, the authors had not the characteristics -either of the thruster to be installed on the considered river cruiser, -or of any tunnel thruster in arrangement with bow of wide-beam vessel.
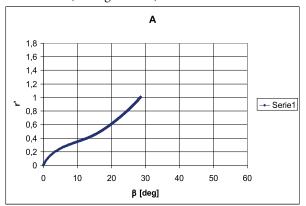
In simulation of most severe manoeuvre when the steering angle of 90 deg was applied to rudder propellers and when the highest value of heeling moment was expected, the bow thruster was set to generate the constant transverse force F_{BT} equal to its rated thrust of 540m kG - the value higher than the highest lateral force at zero ship speed.
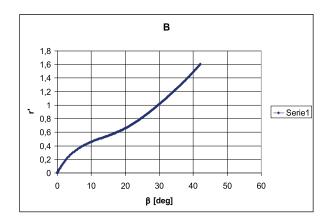
$$
\begin{aligned}
X_{BT} &= 0 \\
Y_{BT} &= F_{BT} \\
N_{BT} &= F_{BT} x_{BT}
\end{aligned}
\tag{9}
$$
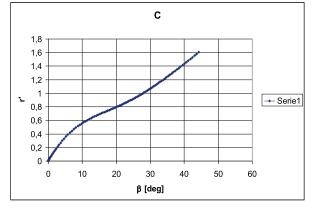
where x_{BT} is the longitudinal coordinate of bow thruster.

RESULTS OF SIMULATIONS

Four manoeuvres were simulated: starboard turning with both rudder-propellers turned to 35 deg (manoeuvre A), 60 deg (B) or 90 deg (C), and starboard turning with propellers turned to 90 deg and operating bow thruster (manoeuvre D). All manoeuvres were started at approach speed of 5.66 m/s (11kn). Simulations were stopped when the limit of applicability of hydrodynamic coefficients was exceeded, i.e. drift angle exceeded 50 deg or non-dimensional yaw rate exceeded value of 1.6. It appeared that at δ = 35deg both parameters remained within limits and the vessel made a closed circle (see Fig.6 and 7).
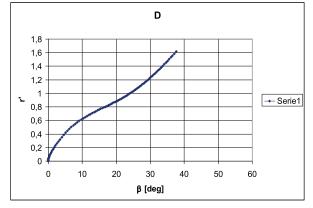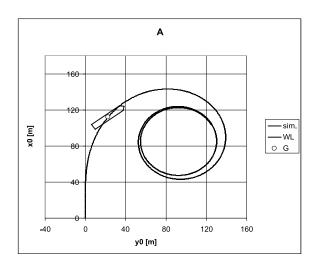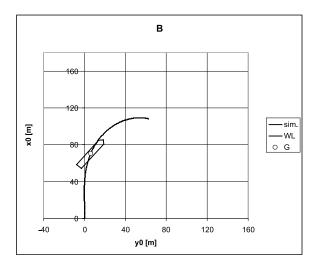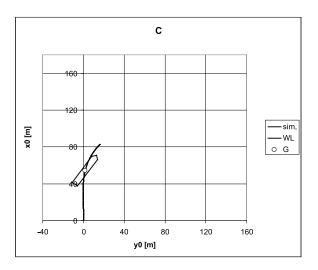
Fig.6. Drift angle β and non-dimensional yaw rate r' during simulated manoeuvres

Fig.7. Trajectory of ship's centre of gravity; position of ship is marked at maximum heeling moment

Fig.8. Forces contributing to heeling moment

Fig.9. Time history of heeling moment

Heeling moment acting on manoeuvring vessel comes from side forces included in the equation of motion (3):

$$m(dv/dt + ur) = -m_y dv/dt - m_x ur + Y_H + Y_P + Y_{BT} \quad (10)$$

where:

$m(dv/dt + ur)$ - is the inertia force on sidewise accelerating or turning ship,

$-m_y dv/dt - m_x ur + Y_H$ - hydrodynamic force, where terms $(-m_y dv/dt - m_x ur)$ come from inertia of added mass,

Y_P - side component of propeller force,

Y_{BT} - bow thruster force.

Because only heeling moment due to manoeuvring motion is considered in this paper, other sources, as e.g. wind, are omitted. According to the conventions presented in Fig.8 the resultant heeling moment is calculated about the Gx axis (at the height of ship's centre of gravity) by using the following formula:
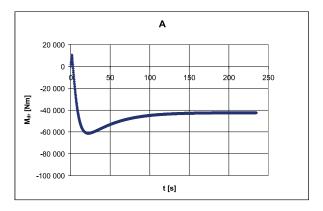
$$M_{dr} = -(-m_y dv/dt - m_x ur + Y_H)z_H - Y_P z_P - Y_{BT} z_{BT} \quad (11)$$
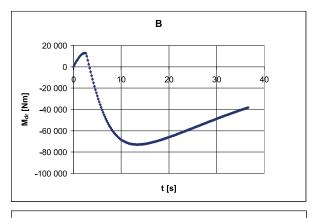
where:

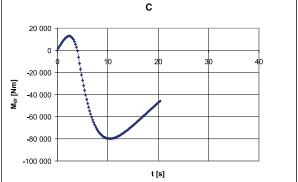z_H - vertical ordinate of application point of hydrodynamic force on ship hull,

z_P - vertical ordinate of propeller axis,

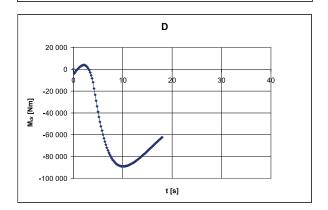z_{BT} - vertical ordinate of the centre of bow thruster outlet.

Time histories of heeling moment during simulated manoeuvres are presented in Fig.9. When the manoeuvre starts a small positive moment appears that tends to heel the ship to starboard. Next the moment due to inertia (centrifugal) forces starts to prevail. The resultant heeling moment becomes negative and tends to heel the ship outwards (to port side). The maximum heeling moment appears some 10 to 25 seconds after the start of manoeuvre, depending on steering angle of rudder-propellers.

In the manoeuvre A the steady circulation with steady velocities and heeling moment was reached after ship made about 2 circles. In the manoeuvres B, C and D the steady motion has not been reached, but one may expect, based on the manoeuvre A, that heeling moment (its absolute value) shall gradually decrease until steady circulation is attained. The extent of simulations is sufficient for the purpose of stability assessment.

In order to prove the assumption of negligible roll motion a simplified analysis of heel angle during turning circle manoeuvre was carried out by using the diagram of righting levers available from standard stability analysis carried out in the framework of design process. The highest value of heeling moment of 89.1 kNm, determined in simulations (Fig.9) was applied. It was assumed that the heeling moment is applied at the beginning of manoeuvre and remains steady. The effect of application of steady heeling moment is illustrated in Fig.10 and Fig.11. Heel angle φ during the simulated manoeuvres shall not exceed the estimated value of dynamic heel angle of 2 deg. In opinion of these authors, neglecting the roll motion in simulations did not affect the manoeuvring motion. One may suggest that the wide-beam, flat-bottomed vessels during tight turning started at full ahead speed shall not be subject to substantial heel angle or roll motion. They may be expected to move like sliding in upright position.
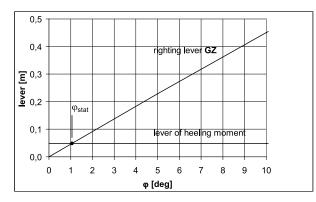

Fig.10. Static heel angle φ_stat of the river cruiser subject to the steady heeling moment of 89.1 kNm

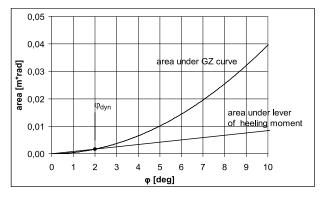*Fig.11. Dynamic heel angle φ_dyn of the river cruiser subject to sudden application of the heeling moment of 89.1 kNm*

CONCLUSIONS

Because the proportions of main dimensions of the considered cruiser are unusual as compared with those of sea going ships, as well as because of wide extent of drift angle and yaw rate, there were no available values of hydrodynamic coefficients. Simulation of turning manoeuvre of small river cruiser propelled and controlled by rudder-propellers required the development of tailor-made model of hydrodynamic forces. Care had to be taken to adjust the scope of applicability of mathematical models to actual parameters of motion during simulated manoeuvres.

The variation of heeling moment during turning reveals that its maximum value appears at the beginning of manoeuvre (change of heading less than 60deg) and, in order to determine data for assessment of ship stability, it is not necessary to extend the mathematical model and to continue simulation until steady turning.

Application of the numerical simulation to non-conventional ships and propulsion/steering systems requires much effort in determination of hydrodynamic and interaction coefficients.

On the other hand, the numerical simulation of ship motion has potential to predict

velocities, accelerations, forces and moments during versatile manoeuvres, and can be useful

not only for testing ship's manoeuvrability but also for assessment of stability.

REFERENCES

1. Directive of the European Parliament and of the Council of 12 December 2006 laying down technical requirements for inland waterway vessels and repealing Council Directive 82/714/EEC (2006/87/EC)

2. Y. Yoshimura: Mathematical Model for Manoeuvring Ship Motion (MMG Model), Workshop on Mathematical Models for Operations involving Ship-Ship Interaction, Tokyo, August 2005

3. H. Yasukawa, N. Hirata, K.K. Koh, K. Punayangkool, K. Kose: Hydrodynamic force characteristics on maneuvering of pusher-barge systems, Journal of Japan Society of Naval Architecture and Ocean Engineering, No. 5, 2?007 (in Japanese)

4. M. W. C. Oosterveld: Wake adapted ducted propellers, NSMB Wageningrn Piubl. No.345, June 1970

5. J. Brix (ed.), Manoeuvring technical manual, Seehafen Verlag GmbH, Hamburg, 1993

CONTACT WITH THE AUTHOR

Jan Kulczyk

Wrocław University of Technology
email: jan.kulczyk@pwr.wroc.pl
POLAND